

Impact in bioconvection MHD Casson nanofluid flow across Darcy-Forchheimer Medium due to nonlinear stretching surface

Humaira Sharif¹, Muzamal Hussain^{*1}, Mohamed A. Khadimallah^{2,3}
Muhammad Nawaz Naeem¹, Hamdi Ayed^{4,5} and Abdelouahed Tounsi^{6,7}

¹ Department of Mathematics, Govt. College University Faisalabad, 38000, Faisalabad, Pakistan

² Prince Sattam Bin Abdulaziz University, College of Engineering, Civil Engineering Department, BP 655, Al-Kharj, 16273, Saudi Arabia

³ Laboratory of Systems and Applied Mechanics, Polytechnic School of Tunisia, University of Carthage, Tunis, Tunisia

⁴ Department of Civil Engineering, College of Engineering, King Khalid University, Abha – 61421, Saudi Arabia

⁵ Higher Institute of Transport and Logistics of Sousse, University of Sousse, Sousse 4023, Tunisia

⁶ YFL (Yonsei Frontier Lab), Yonsei University, Seoul, Korea

⁷ Department of Civil and Environmental Engineering, King Fahd University of Petroleum & Minerals, 31261 Dhahran, Eastern Province, Saudi Arabia

(Received March 18, 2021, Revised August 26, 2021, Accepted September 27, 2021)

Abstract. Current investigation aims to analyze the characteristics of magnetohydrodynamic boundary layer flow of bioconvection Casson fluid in the presence of nano-size particles over a permeable and non-linear stretchable surface. Fluid passes through the Darcy-Forchheimer permeable medium. Effect of different parameter such as Darcy-Forchheimer, porosity parameter, magnetic parameter and Brownian factor are investigated. Increasing Brownian factor leads to the rapid random movement of nanosize particles in fluid flows which shows an expansion in thermal boundary layer and enhances the nanofluid temperature more rapidly. For large values of Darcy-Forchheimer, magnetic parameter and porosity factor the velocity profile decreases. Higher values of velocity slip parameter cause decreasing trend in momentum layer with velocity profile.

Keywords: bio-convection; casson nanofluid; Darcy-Forchheimer flow; energy activation; nonlinear stretching surface; numerical solution; slip boundary conditions

1. Introduction

The suspension of solid materials of size 1-100 nm in an ordinary heat transfer fluids like water or oil, ethylene glycol is commonly known as the nanofluids. These types of nanoparticles are made of distinct materials like Ag , Al_2O_3 and TiO_2 . By using nanofluids, we attained the highest thermal characteristics with lowest concentrations. Recently, nanofluids have been used as the working liquids rather than the base liquids by cause of their huge thermal conductivity. Nano-technology was developed by (Choi and Eastman 1995) and he noted that by including the nanosize particles into the base liquid the heat conductivity of liquids is extended dramatically.

In different processes, to obtain the excellent performance of heat transfer the nanofluids with maximum thermo physical properties are utilized as potential heat transfer liquids. Moreover, nanofluids with particular purpose are utilized in chillers, heating of solar water, domestic refrigerator, cancer therapy and surgery. Lee *et al.* (1999) proved that nanofluids have excellent heat transfer properties as related to base liquids. (Eastman *et al.* 2001)

Utilized the concept of nanofluid and declare that thermal conductivity increased by 40% when copper nanosize particles with volume fraction below 1% are included to oil or ethylene glycol. Buongiorno (2006) used the concept of nanofluids for establishing a mathematical structure that facilitate in analyzing and exploring the thermal properties of liquids along with nanoparticles concentration in base fluids. Bhatti *et al.* (2018) analyzed the mathematical structure of magnetohydrodynamic nanofluid flow including motile microorganisms along chemical reaction and thermal radiation impacts. Yuan with Ma *et al.* (2019) investigated numerically of MHD nanofluid flow in a baffled U-shaped enclosure including magnetic parameter. They noted that local Nusselt number enhance, large values of nanoparticles volume fraction, Rayleigh number and aspect ratio. Abbas *et al.* (2020) studied the second order velocity slip magnetohydrodynamic nanofluid flow with energy activation. Some recent investigations regarding nanofluid can be seen in Ref (Jawad *et al.* 2018, Ahmed *et al.* 2019, Shah *et al.* 2019, Tlili *et al.* 2020, Mishra and Kumar 2020). A large number of non-Newtonian fluid models are defined as rheological characteristics like Maxwell, Carreau, Jeffrey, Oldroyd-B, Casson, Eyring-Powell etc. In all of these structures the powerful model for the suspensions and blood characteristics in daily life is Casson model (Casson 1959). In 1959 the model of Casson fluid was discovered by Casson to determine how pigments of oil suspensions flow (Casson 1959). Salah *et al.* (2019)

*Corresponding author, Ph.D., Research Scholar,
E-mail: muzamal45@gmail.com;
muzamalhussain@gcuf.edu.pk

employed a simple four-variable integral plate theory for examining the thermal buckling properties of functionally graded material (FGM) sandwich plates. The proposed kinematics considers integral terms which include the effect of transverse shear deformations. Material characteristics and thermal expansion coefficient of the ceramic-metal FGM sandwich plate faces are supposed to be graded in the thickness direction according to a “simple power-law” variation in terms of the “volume fractions” of the constituents. The central layer is always homogeneous and consists of an isotropic material. Consider the Soret and Dufour impacts for the purpose of fluid developments. Ramzan *et al.* (2016) investigated the impact of Dufour and Soret on Maxwell mixed convective nanofluid flow via porous stretchable surface. Ghadikolaei *et al.* (2018) analyzed the impact of non-linear thermal radiation on magneto Casson type nanofluid flow including influence of Joule heating through an inclined permeable stretchable surface. Batou *et al.* (2019) studied the wave propagations in sigmoid functionally graded (S-FG) plates using new Higher Shear Deformation Theory (HSDT) based on two-dimensional (2D) elasticity theory. The current higher order theory has only four unknowns, which mean that few numbers of unknowns, compared with first shear deformations and others higher shear deformations theories and without needing shear corrector.

Souayah *et al.* (2019) investigated the numerical solutions of nonlinear radiation on Casson type MHD nanofluid flow through a thin needle. Kumam *et al.* (2019) discussed the entropy Generation applications in MHD Casson nanofluid flow via rotating channels with heat generation/absorption effect. Combine influence of thermal conductivity and variable viscosity on MHD Casson nanofluid along convective velocity and heating slip effects was investigated by Gbadeyan *et al.* (2020). They noted that for higher values of thermal conductivity and variable viscosity, velocity profile increases. Tayeb *et al.* (2020) investigated the incorporation of carbon nanotubes in a polymer matrix makes it possible to obtain nanocomposite materials with exceptional properties. It's in this scientific background that this work was based. Nayak *et al.* (2020) discussed the slip conditions on chemically reactive Casson type nanofluid over a stretchable surface in the presence of motile microorganisms and chemical reaction. Magnetohydrodynamics is the investigation of electrically conducting fluid behavior and magnetic characteristics. Magnetic field effect is very helpful in various chemical and engineering applications of nanofluids. Various equipment like MHD generators, chemical reactions, pumps, geophysical and many others are highly tormented by the Magneto- hydrodynamics effect and also magnetic-electric phenomenon of the liquids. MHD has numerous environmental, industrial and chemical applications in related industries where there are temperature fluctuations. Gafour *et al.* (2020) focused the behavior of non-local shear deformation beam theory for the vibration of functionally graded (FG) nanobeams with porosities that may occur inside the functionally graded materials (FG) during their fabrication, using the non-local differential constitutive relations of Eringen. Bhatti *et al.* (2018) reported the 3D

MHD boundary layer fluid flow having thermal radiations and motile microorganisms by a stretched permeable cylinder. They noted that for higher values of porosity and magnetic parameters, fluid velocity decreases. Effects of convective boundary conditions and yield stress on MHD three- dimensional boundary layer Casson nanofluid flow by a stretchable plate in a permeable media was bestowed by Al-Hossainy *et al.* (2019). Cuong-Le *et al.* (2021) studied a three-dimensional (3D) numerical solution for investigating the free vibration and buckling responses of annular plate, conical and cylindrical shell made of functionally graded (FG) porous rock materials. Isogeometric analysis (IGA) is utilized in order to develop the 3D numerical solution.

Khan *et al.* (2019a, b) investigated the radiative heat flux effect on MHD Jeffrey nanofluid flow subject to thermophoresis and Brownian diffusions. Hayat *et al.* (2020) examined the entropy generation of MHD Jeffrey fluid contain nanoparticles through a stretchable surface with non-linear thermal radiation and energy activation. Ibrahim and Negera (2020) examined the MHD upper-convected Maxwell nanofluid past a stretchable surface with chemical reaction. Few recent researches regarding MHD can be viewed in Ref (Sheikholeslami *et al.* 2014, Daniel *et al.* 2017, Abbas *et al.* 2020). Bestman (1990) was the first researcher to consider the combine chemical reaction performance with Arrhenius energy activation for convective transfer of mass in vertical pipe absorbed with permeable surface. He utilized perturbation technique to attain the analytical results. Le Thanh *et al.* (2020) conducted the bending behavior of porous functionally graded (PFG) micro-plate under the geometrically nonlinear analysis. A small-scale nonlinear solution is established using the Von-Kármán hypothesis and the modified couple stress theory (MCST). To obtain the deflection of the plate, the Reddy higher-order plate theory coupled with isogeometric analysis (IGA) is utilized. Maleque (2013) investigated the heat with mass transfer and free convection magnetohydrodynamic flow by a permeable vertical surface with Arrhenius energy activation and chemical reaction including heat sink/source and viscosity dissipation. Mustafa *et al.* (2017) scrutinized the Buoyancy impacts on magneto-nanofluid flow over a vertical stretching surface including activation energy and chemical reaction effects. They observed that nanoparticles concentration has direct relation to energy activation of chemical reaction and Brownian movement behaviour on concentration in opposite trend to that of thermophoresis force. Hadji (2020) introduced a new higher order shear deformation model is developed for static analysis of functionally graded beams with considering porosities that may possibly occur inside the functionally graded materials (FGMs) during their fabrication.

Irfan *et al.* (2019) investigated the 3D time dependent Carreau nanofluids using the characteristics of chemical reaction with Arrhenius energy activation and non-linear mixed convection. Abbas *et al.* (2020) studied numerically the Hydromagnetic second order velocity slip flow of viscosity along non-linear mixed convection via stretching rotatable disk. Bhatti and Michaelides (2020) analyzed

Arrhenius energy activation on thermo-bioconvected nanofluid flow by a Riga plate. When motile microorganisms which are hefty than water density are extant with nanosize particles in water, bioconvection phenomenon occur because of microorganisms movement in a particular way (Hillesdon *et al.* 1995, Hillesdon and Pedley 1996). Hadji and Safa (2020) developed a hyperbolic shear deformation theory is developed for the bending analysis of softcore and hardcore functionally graded sandwich beams. This theory satisfies the equilibrium conditions at the top and bottom faces of the sandwich beam and does not require the shear correction factor.

The idea of bioconvection nanofluid was first developed by Kuznetsov (2010, 2011a, b). Further, Kuznetsov (2011a, b) developed this concept and focused on nanofluids containing motile microorganisms and he conclude that huge fluid motion caused by gyrotactic microorganisms which are self-propelled increases mixing and avoid agglomeration of nanoparticles in nanofluids. Zuhra *et al.* (2018) analyzed the bioconvection simulation in second grade nanofluid suspension containing motile microorganisms and nanoparticles. Khan *et al.* (2019a, b) analyzed the natural bio-convection flow of a water-based nanofluid with motile microorganisms through a truncated cone along convective conditions. Khan *et al.* (2020) studied the entropy generation investigation in bioconvected nanofluid between two stretching rotatable disks. Recently some researcher used different methods for nonlinear modeling (Tohidi *et al.* 2018, Yeh 2016) and for other structures (AlSaleh and Fuggini 2020, Lee *et al.* 2019, Zahrai and Kakouei 2019, Poplawski *et al.* 2019).

Inspired by all these above-mentioned studies, the main objective of this investigation is to examine the viscous incompressible bioconvection Casson type nanofluid flow with Darcy-Forchheimer resistance across a non-linear stretching surface. Finally, the present results have been related with the previous related literatures to examine the fluctuation in physical quantities of interest.

2. Formulation

We assume viscous incompressible Darcy-Forchheimer Casson type nanofluid flow saturating the permeable media by a nonlinear stretching surface. Moreover, the concentration equation is modified by including chemical reaction and Arrhenius energy activation with fitted constant rate m and reaction rate K_r^2 . The cluster of nanosize particles is ignored, the nanoparticles suspension is assumed to be stable compound that is essential for the presence of motile microorganisms. The surface having stretchable velocity U_w with x-axis and n denotes the non-linearity in surface stretching rate i.e., $u_w(x) = cx^n$. At free surface zero velocity is observed. To emphasize the thermo-physical characteristics, a uniform magnetic field is considered for the fluid. To decline the impact of induced magnetic effect, a small Reynolds number is involved. The x-axis is directed towards the nonlinear stretching surface and y-axis is taken normal to the x-axis. Attributes of

Brownian dissemination and thermophoresis are additionally attended. For an incompressible and isotropic flow the rheological equation of state for Casson type nanofluid is exhibit by Eldabe and Salwa (1995)

$$T_{i,j} = \begin{cases} 2\left(\mu_B + \frac{P_y}{\sqrt{2\pi}}\right)e_{ij}, & \pi > \pi_c \\ 2\left(\mu_B + \frac{P_y}{\sqrt{2\pi_c}}\right)e_{ij}, & \pi < \pi_c \end{cases} \quad (1)$$

Where π denotes the component product of the deformation rate with itself, μ_B is dynamic viscosity of fluid, P_y is the yield fluid stress, π_c is critical value of component product of tensor rate of strain with itself. The governing equations under approximation of boundary layer can be described as (Buongiorno 2006, Haq *et al.* 2014).

$$\frac{\partial u}{\partial x} + \frac{\partial v}{\partial y} = 0, \quad (2)$$

$$\begin{aligned} u \frac{\partial u}{\partial x} + v \frac{\partial u}{\partial y} \\ = \nu \left(1 + \frac{1}{\beta}\right) \frac{\partial^2 u}{\partial y^2} - \left[\frac{\sigma B_0^2}{\rho} - \frac{\nu}{K'}\right] u - \frac{\bar{C}_b}{\sqrt{k}} u^2, \end{aligned} \quad (3)$$

$$\begin{aligned} u \frac{\partial T}{\partial x} + v \frac{\partial T}{\partial y} = \alpha \frac{\partial^2 T}{\partial y^2} + \tau^* \left[\frac{\partial C}{\partial y} \frac{\partial T}{\partial y} D_{Br} + \left(\frac{\partial T}{\partial y}\right)^2 \frac{D_{Th}}{T_\infty} \right] \\ + \frac{\mu}{\rho C_p} \left(1 + \frac{1}{\beta}\right) \left(\frac{\partial u}{\partial y}\right)^2, \end{aligned} \quad (4)$$

$$\begin{aligned} u \frac{\partial C}{\partial x} + v \frac{\partial C}{\partial y} = \frac{D_{Th}}{T_\infty} \frac{\partial^2 T}{\partial y^2} + D_{Br} \frac{\partial^2 C}{\partial y^2} \\ - K_r^2 (C - C_\infty) \left(\frac{T}{T_\infty}\right)^m \exp\left(\frac{-E_a}{k_B T}\right), \end{aligned} \quad (5)$$

$$u \frac{\partial N}{\partial x} + v \frac{\partial N}{\partial y} + \frac{bW_c}{(C_w - C_\infty)} \left[\frac{\partial}{\partial y} \left(N \frac{\partial C}{\partial y}\right)\right] = D_n \left(\frac{\partial^2 N}{\partial y^2}\right), \quad (6)$$

Here, (u, v) are velocities component in (x, y) directions, respectively. The slip boundary conditions are

$$\begin{aligned} u = U_w = cx^n + M_1 \left(1 + \frac{1}{\beta}\right) \frac{\partial u}{\partial y}, \\ T = T_w + M_2 \frac{\partial T}{\partial y}, \quad C = C_w + M_3 \frac{\partial C}{\partial y}, \\ N = N_w + M_4 \frac{\partial N}{\partial y}, \quad v = 0, \quad \text{as } y = 0 \end{aligned} \quad (7)$$

$$u \rightarrow 0, \quad T \rightarrow T_\infty, \quad C \rightarrow C_\infty, \quad N \rightarrow N_\infty, \quad \text{as } y \rightarrow \infty, \quad (8)$$

Where

$$\begin{aligned} M_1(x) = M_0 x^{-\left(\frac{n-1}{2}\right)}, \quad M_2(x) = N_0 x^{-\left(\frac{n-1}{2}\right)}, \\ M_3(x) = L_0 x^{-\left(\frac{n-1}{2}\right)}, \quad M_4(x) = P_0 x^{-\left(\frac{n-1}{2}\right)} \end{aligned}$$

are slip parameters for velocity, temperature, nanoparticles

concentration and microorganism's distributions. M_o, N_o, L_o and P_o are constants. μ is dynamic viscosity, ν is kinematic viscosity, σ is electrical conductivity, ρ is base fluid density, $F = \frac{\bar{c}_b}{\sqrt{k}}$ is inertial factor, K' is permeability coefficient of porous media, τ denotes ratio of nanosize particles heat capacity and heat capacity of base fluid, D_{Br} is Brownian diffusion, α is temperature diffusivity, D_{Th} is thermophoretic effect, $c > 0$ is stretchable rate, $N_\infty, T_\infty, C_\infty$ are ambient microorganisms, thermal and concentration distributions, B_o is magnetic field effect. We considered the following transformation variables

$$\eta = \frac{1}{2} \sqrt{\frac{2\rho c(n+1)}{\mu}} x^{\frac{n-1}{2}} y,$$

$$v = -\frac{1}{2} \sqrt{2cv(n+1)} x^{\frac{n-1}{2}} \left[\frac{(n+1)f + (n-1)f'\eta}{n+1} \right], \quad (9)$$

$$u = cx^n f',$$

$$\theta(\eta)(T_w - T_\infty) = T - T_\infty,$$

$$\phi(\eta)(C_w - C_\infty) = C - C_\infty,$$

$$N(\eta)(N_w - N_\infty) = N - N_\infty,$$

By using the above mentioned transformation in Eqs. (2) to (8), we get

$$f'' + \left(\frac{\beta}{\beta+1}\right) f f'' - Fr \left(\frac{2}{n+1}\right) \left(\frac{\beta}{\beta+1}\right) f'^2$$

$$- M \left(\frac{2}{n+1}\right) \left(\frac{\beta}{\beta+1}\right) f' + \lambda \left(\frac{2}{n+1}\right) \left(\frac{\beta}{\beta+1}\right) f'^2$$

$$- \left(\frac{2n}{n+1}\right) \left(\frac{\beta}{\beta+1}\right) f'^2 = 0, \quad (10)$$

$$\theta'' + Nb Pr \theta' \phi' + Nt Pr \theta'^2 + Pr f \theta'$$

$$+ \left(1 + \frac{1}{\beta}\right) E_c f'^2 = 0, \quad (11)$$

$$\phi'' + \frac{Nt}{Nb} \theta'' + Le Pr f \phi'$$

$$- (Le) Pr \left(\frac{2}{n+1}\right) \gamma^* (1 + \Omega^* \theta)^m \exp\left(\frac{-E}{1 + \Omega^* \theta}\right) \phi = 0, \quad (12)$$

$$N'' + LbfN' - Pe[\phi''(N + \delta_1) + N'\phi'] = 0, \quad (13)$$

$$f(0) = 0, f'(0) = 1 + \alpha \left(1 + \frac{1}{\beta}\right) f''(0), \theta(0)$$

$$= 1 + \gamma \theta'(0), \phi(0) = 1 + \sigma \phi'(0), \quad (14)$$

$$N(0) = 1 + \delta N'(0), \text{ at } \eta = 0,$$

$$f'(\infty) \rightarrow 0, \theta(\infty) \rightarrow 0, \phi(\infty) \rightarrow 0,$$

$$N(\infty) \rightarrow 0, \text{ at } \eta \rightarrow \infty, \quad (15)$$

Here, α is velocity slip parameter, γ is temperature slip parameter, σ is nanoparticles concentration slip parameter, δ is microorganisms slip parameter, M is magnetic parameter, Fr is Forchheimer parameter, λ is porosity parameter, Le is Lewis number, Pr denotes the Prandtl number, Nt is thermophoretic parameter, Nb

denotes the Brownian factor, Ec is Eckert number, λ^* is chemical reaction factor, E denotes energy activation, Lb is bioconvected Lewis number, Pe is bioconvected Peclet number. Mathematically

$$\alpha = M_1 x^{\frac{n-1}{2}} \sqrt{\frac{c(1+n)}{2\nu}}, \quad \gamma = M_2 x^{\frac{n-1}{2}} \sqrt{\frac{c(1+n)}{2\nu}},$$

$$\sigma = M_3 x^{\frac{n-1}{2}} \sqrt{\frac{c(1+n)}{2\nu}}, \quad \delta = M_4 x^{\frac{n-1}{2}} \sqrt{\frac{c(1+n)}{2\nu}},$$

$$M = \frac{\sigma B_o^2}{c\rho x^{n-1}}, \quad Ec = \frac{u_w^2}{c_p(T_w - T_\infty)}, \quad Fr = \frac{x\bar{c}_b}{\sqrt{k}},$$

$$\lambda = \frac{\nu}{K' c x^{n-1}}, \quad Le = \frac{\nu}{D_{Br}}, \quad E = \frac{E_a}{kT_\infty},$$

$$Pr = \frac{\nu}{\alpha}, \quad Nb = \tau D_{Br} (\nu^{-1} C_w - \nu^{-1} C_\infty),$$

$$Nt = \frac{D_{Th}(\tau T_w - \tau T_\infty)}{\nu T_\infty}, \quad \gamma^* = \frac{k_r^2}{c x^{n-1}}, \quad Lb = \frac{\nu}{D_m},$$

$$Pe = \frac{bW_c}{D_m}, \quad \delta_1 = \frac{N_\infty}{N_w - N_\infty},$$

The physical quantities are local motile number, Sherwood number, Nusselt number and skin friction coefficient expressions are defined as

$$N_n = \frac{-x}{(N_w - N_\infty)} \left(\frac{\partial N}{\partial y}\right)_{y=0},$$

$$Shr = \frac{-x}{(C_w - C_\infty)} \left(\frac{\partial C}{\partial y}\right)_{y=0}, \quad (16)$$

$$Nu = \frac{-x}{(T_w - T_\infty)} \left(\frac{\partial T}{\partial y}\right)_{y=0},$$

$$Cf_x = \frac{1}{\rho u_w^2} \left(\mu_\beta \left(1 + \frac{1}{\beta}\right) \left(\frac{\partial u}{\partial y}\right)_{y=0}\right),$$

In terms of non-dimensional variables reduced density number of microorganisms, reduced Sherwood number, reduced Nusselt number and skin friction coefficient are as follows

$$Cf_x Re_x^{\frac{1}{2}} = \left(\frac{n+1}{2}\right)^{\frac{1}{2}} \left(1 + \frac{1}{\beta}\right) f''(0),$$

$$Nu_x Re_x^{-\frac{1}{2}} = -\left(\frac{n+1}{2}\right)^{\frac{1}{2}} \theta'(0), \quad (17)$$

$$Sh_x Re_x^{-\frac{1}{2}} = -\left(\frac{n+1}{2}\right)^{\frac{1}{2}} \phi'(0),$$

$$Nn_x Re_x^{-\frac{1}{2}} = -\left(\frac{n+1}{2}\right)^{\frac{1}{2}} N'(0),$$

Where $Re_x = \frac{xu_w}{\nu}$ denotes the Reynolds number.

3. Solutions method

The RK (Runge-Kutta) method is widely used for determining the initial-value problems. RK method is very stable, self-starting and very easy to implement. The nonlinear differential Eqs. (10) to (15) along boundary conditions constitute two point BVP (Boundary value

problem) are tackled numerically by applying RK method, in this technique the system of Eqs. (10) to (15) is reduced to first order ODE (Ordinary differential equations).

$$\begin{aligned}
 y_1' &= y_1 \\
 y_1'' &= y_2 \\
 y_1''' &= y_2 = y_3 \\
 y_3' &= \left(\frac{\beta}{\beta+1}\right) \left[\begin{aligned} &Fr \left(\frac{2}{n+1}\right) y_2^2 - y_1 y_3 \\ &+ M \left(\frac{2}{n+1}\right) y_2 + \lambda \left(\frac{2}{n+1}\right) y_2 \\ &+ \left(\frac{2n}{n+1}\right) y_2^2 \end{aligned} \right] \\
 y_4' &= y_4 \\
 y_4'' &= y_5 \\
 y_5' &= -Pr[y_1 y_5 + Nb y_5 y_7 + Nt y_5^2] - \left(1 + \frac{1}{\beta}\right) Ec y_3^2 \\
 y_6' &= y_6 \\
 y_6'' &= y_7 \\
 y_7' &= Le Pr y_1 y_7 - \left(\frac{Nt}{Nb}\right) y_5' + Le Pr \left(\frac{2}{n+1}\right) \gamma^* \\
 &\quad \left(1 + \Omega^* y_4\right)^m \exp\left(\frac{-E}{1 + \Omega^* y_4}\right) y_6 \\
 y_8' &= y_8 \\
 y_8'' &= y_9 \\
 y_9' &= -Lb y_1 y_9 + Pe[(y_8 + \delta_1) y_7' + y_7 y_9]
 \end{aligned}$$

With the transformed conditions (14) and (15)

$$\begin{aligned}
 y_1(0) &= 0, \quad y_2(0) = 1 + \alpha \left(1 + \frac{1}{\beta}\right) y_3(0), \\
 y_4(0) &= 1 + \gamma y_5(0), \quad y_6(0) = 1 + \sigma y_7(0), \\
 y_8(0) &= 1 + \delta y_9(0), \quad \text{as } \eta \rightarrow 0 \\
 y_2(\infty) &\rightarrow 0, \quad y_4(\infty) \rightarrow 0, \quad y_6(\infty) \rightarrow 0, \\
 y_8(\infty) &\rightarrow 0, \quad \text{as } \eta \rightarrow \infty
 \end{aligned}$$

For the residual of continuous outcomes erratum control and mesh section provided for all the calculations.

4. Result and discussion

The non-linear ODE's (10) to (13) subject to associated boundary conditions are integrated numerically by utilizing a shooting technique. Effects of distinct parameters on flow

Table 1 Comparison of results for $-\theta'(0)$ with distinct values of Pr, when $\beta \rightarrow \infty, n = 1, Fr = \lambda = M = Nb = Nt = \alpha = \gamma = \sigma = \delta = Le = Pe = Lb = Ec = 0$

| Pr | Khan and Pop (2010) | Present results |
|-------|---------------------|-----------------|
| 0.20 | 0.1691 | 0.1691 |
| 0.70 | 0.4539 | 0.4539 |
| 2.00 | 0.9113 | 0.9113 |
| 7.00 | 1.8954 | 1.8954 |
| 20.00 | 3.3539 | 3.3539 |
| 70.00 | 6.4621 | 6.4621 |

distributions are shown in Figs. 1 to 5. The impact of Forchheimer variable Fr on momentum profile f' is portrayed in Fig. 1. For maximum values of Fr shows decreasing behavior of f' . Physically, the strong resistance offered to the flow of the fluid results in decreasing behavior of flow momentum and also reduces the correlated boundary layer. Fig. 2 displayed the impact of porosity parameter λ on momentum profile f' . It is noted that by upgrading the λ shows that momentum profile f' and associated energy layer are decreases. The existence of

Table 2 Comparison results for Nusselt number with distinct values of Nb and Nt for $\beta \rightarrow \infty, n = 1, Fr = \lambda = M = \alpha = \gamma = \sigma = \delta = Pe = Lb = Ec = 0, Pr = Le = 10$

| Nb | Nt | Khan and Pop (2010) | Present results |
|------|------|---------------------|-----------------|
| 0.10 | 0.1 | 0.9524 | 0.9524 |
| | 0.2 | 0.6932 | 0.6932 |
| | 0.3 | 0.5201 | 0.5201 |
| 0.20 | 0.1 | 0.5056 | 0.5056 |
| | 0.2 | 0.3654 | 0.3654 |
| | 0.3 | 0.2731 | 0.2731 |

Table 3 Comparison results for Sherwood number with distinct values of Nb and Nt for $\beta \rightarrow \infty, n = 1, Fr = \lambda = M = \alpha = \gamma = \sigma = \delta = Pe = Lb = Ec = 0, Pr = Le = 10$

| Nb | Nt | Khan and Pop (2010) | Present results |
|------|------|---------------------|-----------------|
| 0.10 | 0.1 | 2.1294 | 2.1294 |
| | 0.2 | 2.2740 | 2.2740 |
| | 0.3 | 2.5286 | 2.5286 |
| 0.20 | 0.1 | 2.3819 | 2.3819 |
| | 0.2 | 2.5152 | 2.5152 |
| | 0.3 | 2.6555 | 2.6555 |

Table 4 Numerical values of skin-friction for distinct values of parameters

| α | Fr | λ | β | $C_{fx}(0)$ |
|----------|------|-----------|---------|-------------|
| 0.0 | | | | -1.5999 |
| 0.3 | 0.1 | 0.1 | 0.2 | -0.7659 |
| 0.6 | | | | -0.2700 |
| | 0.0 | | | -0.5768 |
| 0.2 | 0.3 | | | -0.5881 |
| | 0.6 | | | -0.5983 |
| | | 0.0 | | -0.5682 |
| 0.2 | | 0.3 | | -0.6033 |
| | | 0.6 | | -0.6323 |
| | | | 0.4 | -0.5138 |
| | | | 0.6 | -0.4810 |
| | | | 0.8 | -0.4609 |

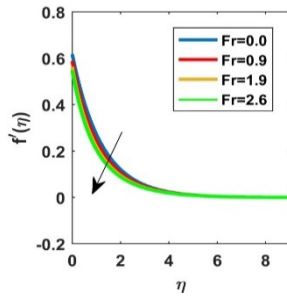


Fig. 1 Velocity profile for variation of Forchheimer variable Fr

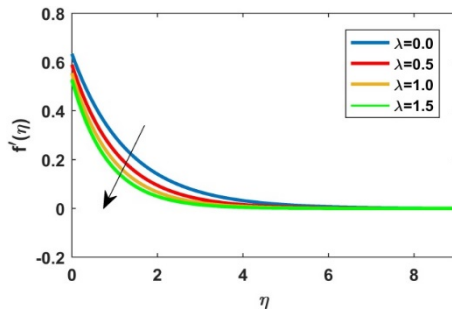


Fig. 2 Velocity profile for variation of porosity parameter λ

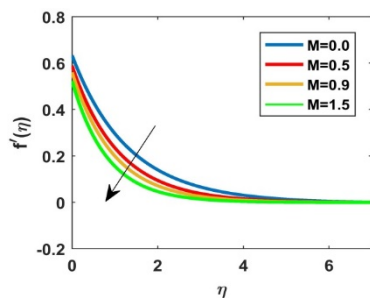


Fig. 3 Velocity profile for variation of magnetic parameter M

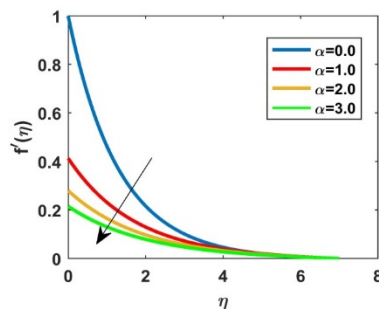


Fig. 4 Velocity profile for variation of α

permeable space enhances the protection from fluid stream which reveals to bringing down fluid movement and its associated energy layer. Fig. 3 shows the impact of magnetic parameter M on velocity field f' . Physically, intensive and strong Lorentz force developed by MHD conclusion in sudden bumps and reduction in directions of fluid flow, which leads to a reduction behavior in velocity

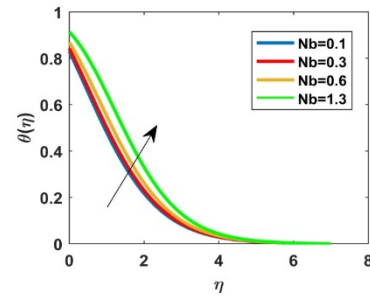


Fig. 5 Temperature profile for variation of Brownian diffusion parameter Nb

field. The influence of velocity slip parameter α on velocity profile f' is presents in Fig. 4. Higher values of α cause decreasing trend in momentum layer with velocity profile f' . The impact of Brownian diffusion parameter on thermal profile θ is demonstrates in Fig. 5. Tables 1, 2 and 3 displayed to validate the current solutions with previous published literature in specific cases. We noted that present results have excellent agreement with previous results by Khan and Pop (2010) in specific case. From Table 4, it is clear that for large values of velocity slip parameter and Casson parameter the numerical values of skin friction coefficient increase.

5. Conclusions

The steady incompressible Darcy-Forchheimer boundary layer flow of MHD bioconvection Casson type nanofluid by nonlinear stretchable surface with slip conditions, Arrhenius energy activation and chemical reaction has been investigated numerically. The impact of distinct parameters is examined via tables and graphs. The validity of the current investigation is authorized through comparing the existing outcomes with previous published literature. For large values of Darcy-Forchheimer Fr , magnetic parameter M and porosity factor λ the velocity profile decreases. Higher values of α cause decreasing trend in momentum layer with velocity profile. Increasing Nb leads to the rapid random movement of nanosize particles in fluid flows which shows an expansion in thermal boundary layer and enhances the nanofluid temperature more rapidly. The bioconvection may provide stability to enhance heat transportation.

Declaration of conflicting interests

The authors declared no potential conflicts of interest with respect to the research, authorship, and/or publication of this article.

Acknowledgments

The authors extend their appreciation to the Deanship of Scientific Research at King Khalid University for funding this work through research groups under grant number RGP.1/154/42.

ORCID ID

Muzamal Hussain

<http://orcid.org/0000-0002-6226-359X>

References

- Abbas, S.Z., Khan, M.I., Kadry, S., Khan, W.A., Israr-Ur-Rehman, M. and Waqas, M. (2020), "Fully developed entropy optimized second order velocity slip MHD nanofluid flow with activation energy", *Comput. Methods Programs Biomed.*, **190**, 105362. <https://doi.org/10.1016/j.cmpb.2020.105362>
- Ahmed, Z., Nadeem, S., Saleem, S. and Ellahi, R. (2019), "Numerical study of unsteady flow and heat transfer CNT-based MHD nanofluid with variable viscosity over a permeable shrinking surface", *Int. J. Numer. Methods Heat & Fluid Flow*. <https://doi.org/10.1108/HFF-04-2019-0346>
- Al-Hossainy, A.F., Eid, M.R. and Zoromba, M.S. (2019), "SQLM for external yield stress effect on 3D MHD nanofluid flow in a porous medium", *Physica Scripta*, **94**(10), 105208. <https://doi.org/10.1088/1402-4896/ab2413>
- AlSaleh, R.J. and Fuggini, C. (2020), "Combining GPS and accelerometers' records to capture torsional response of cylindrical tower", *Smart Struct. Syst., Int. J.*, **25**(1), 111-122. <https://doi.org/10.12989/sss.2020.25.1.111>
- Batou, B., Nebab, M., Bennai, R., Atmane, H.A., Tounsi, A. and Bouremana, M. (2019), "Wave dispersion properties in imperfect sigmoid plates using various HSDTs", *Steel Compos. Struct., Int. J.*, **33**(5), 699-716. <https://doi.org/10.12989/scs.2019.33.5.699>
- Bestman, A.V. (1990), "Natural convection boundary layer with suction and mass transfer in a porous medium", *Int. J. Energy Res.*, **14**(4), 389-396. <https://doi.org/10.1002/er.4440140403>
- Bhatti, M.M. and Michaelides, E.E. (2020), "Study of Arrhenius activation energy on the thermo-bioconvection nanofluid flow over a Riga plate", *J. Thermal Anal. Calorimetry*, 1-10. <https://doi.org/10.1007/s10973-020-09492-3>
- Bhatti, M.M., Mishra, S.R., Abbas, T. and Rashidi, M.M. (2018), "A mathematical model of MHD nanofluid flow having gyrotactic microorganisms with thermal radiation and chemical reaction effects", *Neural Comput. Applicat.*, **30**(4), 1237-1249. <https://doi.org/10.1007/s00521-016-2768-8>
- Buongiorno, J. (2006), "Convective transport in nanofluids", *J. Heat Transfer*, **128**(3), 240-250.
- Casson, N.A. (1959), "Flow equation for pigment oil suspensions of the printing ink type", In: *Rheology of Dispersed System*, Peragamon Press. <https://doi.org/10.1002/9781444391060>
- Choi, S.U. and Eastman, J.A. (1995), "Enhancing thermal conductivity of fluids with nanoparticles", (No. ANL/MSD/CP-84938; CONF-951135-29), Argonne National Lab., IL, USA.
- Cuong-Le, T., Nguyen, K.D., Nguyen-Trong, N., Khatir, S., Nguyen-Xuan, H. and Abdel-Wahab, M. (2021), "A three-dimensional solution for free vibration and buckling of annular plate, conical, cylinder and cylindrical shell of FG porous-cellular materials using IGA", *Compos. Struct.*, **259**, 113216. <https://doi.org/10.1016/j.compstruct.2020.113216>
- Daniel, Y.S., Aziz, Z.A., Ismail, Z. and Salah, F. (2017), "Effects of thermal radiation, viscous and Joule heating on electrical MHD nanofluid with double stratification", *Chinese J. Phys.*, **55**(3), 630-651. <https://doi.org/10.1016/j.cjph.2017.04.001>
- Eldabe, N.T.M. and Salwa, M.G.E. (1995), "Heat transfer of MHD non-Newtonian Casson fluid flow between two rotating cylinders", *J. Phys.*, **64**, 41-64.
- Eastman, J.A., Choi, S.U.S., Li, S., Yu, W. and Thompson, L.J. (2001), "Anomalously increased effective thermal conductivities of ethylene glycol-based nanofluids containing copper nanoparticles", *Appl. Phys. Lett.*, **78**(6), 718-720. <https://doi.org/10.1063/1.1341218>
- Gafour, Y., Hamidi, A., Benahmed, A., Zidour, M., & Bensattalah, T. (2020), "Porosity-dependent free vibration analysis of FG nanobeam using non-local shear deformation and energy principle", *Adv. Nano Res., Int. J.*, **8**(1), 37-47. <https://doi.org/10.12989/anr.2020.8.1.037>
- Gbadeyan, J.A., Titiloye, E.O. and Adeosun, A.T. (2020), "Effect of variable thermal conductivity and viscosity on Casson nanofluid flow with convective heating and velocity slip", *Heliyon*, **6**(1), e03076. <https://doi.org/10.1016/j.heliyon.2019.e03076>
- Ghadikolaei, S.S., Hosseinzadeh, K., Ganji, D.D. and Jafari, B. (2018), "Nonlinear thermal radiation effect on magneto Casson nanofluid flow with Joule heating effect over an inclined porous stretching sheet", *Case Studies Thermal Eng.*, **12**, 176-187. <https://doi.org/10.1016/j.csite.2018.04.009>
- Hadji, L. (2020), "Influence of the distribution shape of porosity on the bending of FGM beam using a new higher order shear deformation model", *Smart Struct. Syst., Int. J.*, **26**(2), 253-262. <https://doi.org/10.12989/sss.2020.26.2.253>
- Hadji, L. and Safa, A. (2020), "Bending analysis of softcore and hardcore functionally graded sandwich beams", *Earthq. Struct., Int. J.*, **18**(4), 481-492. <https://doi.org/10.12989/eas.2020.18.4.481>
- Haq, R.U., Nadeem, S., Khan, Z.H. and Okedayo, T.G. (2014), "Convective heat transfer and MHD effects on Casson nanofluid flow over a shrinking sheet", *Central Eur. J. Phys.*, **12**(12), 862-871. <https://doi.org/10.2478/s11534-014-0522-3>
- Hayat, T., Kanwal, M., Qayyum, S. and Alsaedi, A. (2020), "Entropy generation optimization of MHD Jeffrey nanofluid past a stretchable sheet with activation energy and non-linear thermal radiation", *Physica A: Statist. Mech. Applicat.*, **544**, 123437. <https://doi.org/10.1016/j.physa.2019.123437>
- Hillesdon, A.J. and Pedley, T.J. (1996), "Bioconvection in suspensions of oxytactic bacteria: linear theory", *J. Fluid Mech.*, **324**, 223-259. <https://doi.org/10.1017/S0022112096007902>
- Hillesdon, A.J., Pedley, T.J. and Kessler, J.O. (1995), "The development of concentration gradients in a suspension of chemotactic bacteria", *Bull. Math. Biol.*, **57**, 299-344. <https://doi.org/10.1007/BF02460620>
- Ibrahim, W. and Negera, M. (2020), "MHD slip flow of upper-convected Maxwell nanofluid over a stretching sheet with chemical reaction", *J. Egypt. Mathe. Soc.*, **28**(1), 1-28. <https://doi.org/10.1186/s42787-019-0057-2>
- Irfan, M., Khan, W.A., Khan, M. and Gulzar, M.M. (2019), "Influence of Arrhenius activation energy in chemically reactive radiative flow of 3D Carreau nanofluid with nonlinear mixed convection", *J. Phys. Chem. Solids*, **125**, 141-152. <https://doi.org/10.1016/j.jpcs.2018.10.016>
- Jawad, M., Shah, Z., Islam, S., Bonyah, E. and Khan, A.Z. (2018), "Darcy-Forchheimer flow of MHD nanofluid thin film flow with Joule dissipation and Navier's partial slip", *J. Phys. Commun.*, **2**(11), 115014. <https://doi.org/10.1088/2399-6528/aaeddf>
- Khan, W.A. and Pop, I. (2010), "Boundary-layer flow of a nanofluid past a stretching sheet", *Int. J. Heat Mass Transfer*, **53**(11-12), 2477-2483.
- Khan, M.I., Hayat, T., Waqas, M., Alsaedi, A. and Khan, M.I. (2019a), "Effectiveness of radiative heat flux in MHD flow of Jeffrey-nanofluid subject to Brownian and thermophoresis diffusions", *J. Hydrodyn.*, **31**(2), 421-427. <https://doi.org/10.1007/s42241-019-0003-7>
- Khan, W.A., Rashad, A.M., Abdou, M.M.M. and Tlili, I. (2019b), "Natural bioconvection flow of a nanofluid containing gyrotactic microorganisms about a truncated cone", *Eur. J.*

- Mech. – B/Fluids*, **75**, 133-142.
<https://doi.org/10.1016/j.euromechflu.2019.01.002>
- Khan, N.S., Shah, Q., Bhaumik, A., Kumam, P., Thounthong, P. and Amiri, I. (2020), “Entropy generation in bioconvection nanofluid flow between two stretchable rotating disks”, *Scientific Reports*, **10**(1), 1-26.
<https://doi.org/10.1038/s41598-020-61172-2>
- Kumam, P., Shah, Z., Dawar, A., Rasheed, H.U. and Islam, S. (2019), “Entropy generation in MHD radiative flow of CNTs Casson nanofluid in rotating channels with heat source/sink”, *Mathe. Problems Eng.* <https://doi.org/10.1155/2019/9158093>
- Kuznetsov, A.V. (2010), “The onset of nanofluid bioconvection in a suspension containing both nanoparticles and gyrotactic microorganisms”, *Int. Commun. Heat Mass Transfer*, **37**, 1421-1425. <https://doi.org/10.1016/j.icheatmasstransfer.2010.08.015>
- Kuznetsov, A.V. (2011a), “Non-oscillatory and oscillatory nanofluid bio-thermal convection in a horizontal layer of finite depth”, *Eur. J. Mech. – B/Fluids*, **30**, 156-165.
<https://doi.org/10.1016/j.euromechflu.2010.10.007>
- Kuznetsov, A.V. (2011b), “Nanofluid bioconvection in water-based suspensions containing nanoparticles and oxytactic microorganisms: oscillatory instability”, *Nanoscale Res. Lett.*, **6**, 100. <https://doi.org/10.1186/1556-276X-6-100>
- Le Thanh, C., Nguyen, T.N., Vu, T.H., Khatir, S. and Wahab, M.A. (2020), “A geometrically nonlinear size-dependent hypothesis for porous functionally graded micro-plate”, *Eng. Comput.*, 1-12. <https://doi.org/10.1007/s00366-020-01154-0>
- Lee, S., Choi, S.U.S., Li, S. and Eastman, J.A. (1999), “Measuring thermal conductivity of fluids containing oxide nanoparticles”, *J. Heat Transfer*, **121**(2), 280e289.
<https://doi.org/10.1115/1.2825978>
- Lee, S.Y., Huynh, T.C., Dang, N.L. and Kim, J.T. (2019), “Vibration characteristics of caisson breakwater for various waves, sea levels, and foundations”, *Smart Struct. Syst., Int. J.*, **24**(4), 525-539. <https://doi.org/10.12989/sss.2019.24.4.525>
- Ma, Y., Mohebbi, R., Rashidi, M.M., Yang, Z. and Sheremet, M.A. (2019), “Numerical study of MHD nanofluid natural convection in a baffled U-shaped enclosure”, *Int. J. Heat Mass Transfer*, **130**, 123-134.
<https://doi.org/10.1016/j.ijheatmasstransfer.2018.10.072>
- Maleque, K. (2013), “Effects of binary chemical reaction and activation energy on MHD boundary layer heat and mass transfer flow with viscous dissipation and heat generation/absorption”, *ISRN Thermodyn.*
<https://doi.org/10.1155/2013/284637>
- Mishra, A. and Kumar, M. (2020), “Velocity and thermal slip effects on MHD nanofluid flow past a stretching cylinder with viscous dissipation and Joule heating”, *SN Appl. Sci.*, **2**(8), 1-13.
<https://doi.org/10.1007/s42452-020-3156-7>
- Mustafa, M., Khan, J.A., Hayat, T. and Alsaedi, A. (2017), “Buoyancy effects on the MHD nanofluid flow past a vertical surface with chemical reaction and activation energy”, *Int. J. Heat Mass Transfer*, **108**, 1340-1346.
<https://doi.org/10.1016/j.ijheatmasstransfer.2017.01.029>
- Nayak, M.K., Prakash, J., Tripathi, D., Pandey, V.S., Shaw, S. and Makinde, O.D. (2020), “3D Bioconvective multiple slip flow of chemically reactive Casson nanofluid with gyrotactic microorganisms”, *Heat Transfer—Asian Res.*, **49**(1), 135-153.
<https://doi.org/10.1002/htj.21603>
- Poplawski, B., Mikulowski, G., Pisarski, D., Wiszowaty, R. and Jankowski, L. (2019), “Optimum actuator placement for damping of vibrations using the Prestress-Accumulation Release control approach”, *Smart Struct. Syst., Int. J.*, **24**(1), 27-35. <https://doi.org/10.12989/sss.2019.24.1.027>
- Ramzan, M., Bilal, M., Chung, J.D. and Farooq, U. (2016), “Mixed convective flow of Maxwell nanofluid past a porous vertical stretched surface—An optimal solution”, *Results Phys.*, **6**, 1072-1079. <https://doi.org/10.1016/j.rinp.2016.11.036>
- Salah, F., Boucham, B., Bourada, F., Benzair, A., Bousahla, A.A. and Tounsi, A. (2019), “Investigation of thermal buckling properties of ceramic-metal FGM sandwich plates using 2D integral plate model”, *Steel Compos. Struct., Int. J.*, **33**(6), 805-822. <https://doi.org/10.12989/scs.2019.33.6.805>
- Shah, Z., Dawar, A., Kumam, P., Khan, W. and Islam, S. (2019), “Impact of nonlinear thermal radiation on MHD nanofluid thin film flow over a horizontally rotating disk”, *Appl. Sci.*, **9**(8), 1533. <https://doi.org/10.3390/app9081533>
- Sheikholeslami, M., Abelman, S. and Ganji, D.D. (2014), “Numerical simulation of MHD nanofluid flow and heat transfer considering viscous dissipation”, *Int. J. Heat Mass Transfer*, **79**, 212-222.
<https://doi.org/10.1016/j.ijheatmasstransfer.2014.08.004>
- Souayah, B., Reddy, M.G., Sreenivasulu, P., Poornima, T., Rahimi-Gorji, M. and Alarifi, I.M. (2019), “Comparative analysis on non-linear radiative heat transfer on MHD Casson nanofluid past a thin needle”, *J. Molecular Liquids*, **284**, 163-174.
<https://doi.org/10.1016/j.molliq.2019.03.151>
- Tayeb, T.S., Zidour, M., Bensattalah, T., Heireche, H., Benahmed, A. and Bedia, E.A. (2020), “Mechanical buckling of FG-CNTs reinforced composite plate with parabolic distribution using Hamilton’s energy principle”, *Adv. Nano Res., Int. J.*, **8**(2), 135-148. <https://doi.org/10.12989/anr.2020.8.2.135>
- Tlili, I., Ramzan, M., Kadry, S., Kim, H.W. and Nam, Y. (2020), “Radiative mhd nanofluid flow over a moving thin needle with entropy generation in a porous medium with dust particles and hall current”, *Entropy*, **22**(3), 354.
<https://doi.org/10.3390/e22030354>
- Tohidi, H., Hosseini-Hashemi, S.H. and Maghsoudpour, A. (2018), “Size-dependent forced vibration response of embedded micro cylindrical shells reinforced with agglomerated CNTs using strain gradient theory”, *Smart Struct. Syst., Int. J.*, **22**(5), 527-546. <https://doi.org/10.12989/sss.2018.22.5.527>
- Wang, C.Y. (1889), “Free convection on a vertical stretching surface”, *J. Appl. Math. Mech. (ZAMM)*, **69**, 418-420.
<https://doi.org/10.1002/zamm.19890691115>
- Yeh, J.Y. (2016), “Vibration characteristic analysis of sandwich cylindrical shells with MR elastomer”, *Smart Struct. Syst., Int. J.*, **18**(2), 233-247. <https://doi.org/10.12989/sss.2016.18.2.233>
- Zahrai, S.M. and Kakouei, S. (2019), “Shaking table tests on a SDOF structure with cylindrical and rectangular TLDs having rotatable baffles”, *Smart Struct. Syst., Int. J.*, **24**(3), 391-401.
<https://doi.org/10.12989/sss.2019.24.3.391>
- Zuhra, S., Khan, N.S., Shah, Z., Islam, S. and Bonyah, E. (2018), “Simulation of bioconvection in the suspension of second grade nanofluid containing nanoparticles and gyrotactic microorganisms”, *AIP Adv.*, **8**(10), 105210.
<https://doi.org/10.1063/1.5054679>